This is a preprint, the final version is subject to change, of the American Mineralogist (MSA)
Cite as Authors (Year) Title. American Mineralogist, in press.
DOI: https://doi.org/10.2138/am-2020-7467

Revision 1

The chlorine-isotopic composition of lunar KREEP from magnesian-suite troctolite 76535

Francis M. McCubbin[1*] and Jessica J. Barnes[1,2]

*Corresponding author: francis.m.mccubbin@nasa.gov

[1]NASA Johnson Space Center, Mailcode XI, 2101 NASA Parkway, Houston, TX 77058, USA.

[2]Lunar and Planetary Laboratory, University of Arizona, 1629 E University Blvd, Tucson, AZ 85721, USA.

Abstract – We conducted *in-situ* Cl isotopic measurements of apatite within intercumulus regions and within a holocrystalline olivine-hosted melt inclusion in magnesian-suite troctolite 76535 from Apollo 17. These data were collected to place constraints on the Cl-isotopic composition of the last liquid to crystallize from the lunar magma ocean (i.e., *ur*KREEP, named after its enrichments in incompatible lithophile trace elements like potassium, rare earth elements, and phosphorus). The apatite in the olivine-hosted melt inclusion and within the intercumulus regions of the sample yielded Cl-isotopic compositions of 28.3 ± 0.9 ‰ (2σ) and 30.3 ± 1.1 ‰ (2σ), respectively. The concordance of these values from both textural regimes we analyzed indicates that the Cl-isotopic composition of apatites in 76535 likely represents the Cl-isotopic composition of the KREEP-rich magnesian-suite magmas. Based on the age of 76535, these results imply that the KREEP reservoir attained a Cl-isotopic composition of 28–30 ‰ by at least 4.31 Ga, consistent with the onset of Cl-isotopic fractionation at the time of lunar magma ocean crystallization or shortly thereafter. Moreover, lunar samples that yield Cl-isotopic compositions higher than the value for KREEP are likely affected by secondary processes such as impacts and/or magmatic degassing. The presence of KREEP-rich olivine-hosted melt inclusions within one of the most pristine and ancient KREEP-rich rocks from the Moon provides a new opportunity to characterize the geochemistry of KREEP. In particular, a broader analysis of stable isotopic compositions of highly and moderately volatile elements could provide an unprecedented advancement in our characterization of the geochemical composition of the KREEP reservoir and of volatile-depletion processes during magma ocean crystallization, more broadly.

Keywords – Apatite, Mg-suite, Apollo, Volatiles, Moon, magma ocean, melt inclusion, phosphates

Introduction

The Moon formed in the aftermath of a giant impact between the proto-Earth and Theia (Canup and Asphaug, 2001; Hartmann and Davis, 1975; Lock et al., 2018) between 60 and 120 million years (Touboul et al., 2007) after the birth of the Solar System at 4.567 Ga (as defined by the ages of calcium-aluminum rich inclusions within CV meteorites; Connelly et al., 2012). After the Moon coalesced into a distinct body, it underwent differentiation to form a small metallic core and molten silicate mantle, the latter of which is referred to as the lunar magma ocean (LMO). As cooling proceeded, the LMO crystallized to form a cumulate mantle comprised of mostly ferromagnesian silicates with progressively higher Mg/Fe ratios with depth (Charlier et al., 2018; Elardo et al., 2011; Elkins-Tanton and Grove, 2011; Lin et al., 2017; Rapp and Draper, 2018; Snyder et al., 1992). The LMO liquid became progressively enriched in Fe and incompatible trace elements as crystallization continued, and a primary flotation crust of ferroan anorthosite formed after about 70–80% crystallization (Charlier et al., 2018; Elkins-Tanton and Grove, 2011; Lin et al., 2017; Rapp and Draper, 2018; Snyder et al., 1992). After 88–98% crystallization, the upper part of the cumulate mantle became rich in Fe-Ti oxide cumulates (Charlier et al., 2018; Elkins-Tanton and Grove, 2011; Lin et al., 2017; Rapp and Draper, 2018; Snyder et al., 1992), and the final residual liquid that remained uncrystallized after about 99% crystallization was enriched in incompatible elements and termed *ur*KREEP (Warren, 1988; Warren and Wasson, 1979) after the incompatible elements potassium (K), rare earth elements (REE), and phosphorus (P). The abundance of cool, dense, Fe-rich cumulates at the top of the mantle and hot Fe-poor cumulates at the base of the lunar mantle resulted in a density instability that instigated cumulate mantle overturn (Hess and Parmentier, 1995; Ringwood and Kesson, 1976), resulting in a redistribution

of cumulates in the lunar mantle that set the stage for secondary crust production on the Moon (Shearer et al., 2006; Wieczorek et al., 2006).

The fate of *ur*KREEP during cumulate mantle overturn is poorly constrained, but a KREEP-like component in products of secondary volcanism is evident in many lunar sample types including plutonic rocks from the lunar highlands, some mare basalts, and some impact melt rocks (Shearer et al., 2006). A pure sample of *ur*KREEP is not preserved in any lunar samples, so the composition of *ur*KREEP must be inferred from samples with a KREEP component (Taylor et al., 2006; Warren, 1988; Warren and Wasson, 1979). Given that *ur*KREEP represents a primordial geochemical reservoir on the Moon, establishing its isotopic and chemical composition is important for constraining geochemical mixing models and for determining the bulk composition of the Moon, particularly for the origin and onset of moderately and highly volatile element depletion in the Moon (Barnes et al., 2016; Boyce et al., 2018; Day and Moynier, 2014; Day et al., 2020; Dhaliwal et al., 2018; Hauri et al., 2015; Kato et al., 2015; Lock et al., 2018; McCubbin et al., 2015; Wang and Jacobsen, 2016). In particular, chlorine is one of the most incompatible moderately volatile elements, so the Cl-isotopic composition of KREEP represents the isotopic composition of the largest Cl reservoir on the Moon at the end of LMO crystallization (Boyce et al., 2018; McCubbin et al., 2015). Defining the Cl-isotopic composition of KREEP among the range of Cl-isotopic compositions in lunar samples will establish primary from secondary Cl-isotopic signatures and could be used to establish mixing models between KREEP and non-KREEP geochemical reservoirs (e.g., Boyce et al., 2018).

The Cl-isotopic compositions of lunar samples range from -4‰ to +81‰ (Barnes et al., 2019; Barnes et al., 2016; Boyce et al., 2015; Potts et al., 2018; Sharp et al., 2010; Stephant et al., 2019; Tartèse et al., 2014a; Treiman et al., 2014; Wang et al., 2019), but estimates of the Cl isotopic

composition of KREEP range from 25‰ to 33‰ (Barnes et al., 2016; Boyce et al., 2018; Treiman et al., 2014). The oldest KREEP-rich rocks crystallized in the lunar highlands at 4.31–4.39 Ga (Borg et al., 2015; Shearer et al., 2015) and are members of the magnesian suite. The magnesian suite is a series of plutonic mafic-ultramafic cumulates whose parental liquids are thought to have formed through low-degree partial melting of a hybridized cumulate source at the base of the lunar crust containing ferroan anorthosites, early-formed Mg-rich LMO cumulates, and KREEP (Hess, 1994; Shearer et al., 2015; Shearer and Papike, 2005). Given their ancient ages and minimal contribution from late-stage Fe-rich LMO cumulates to their parental magmas, the magnesian-suite are thought to represent our best samples to characterize volatiles, including the isotopic composition of Cl, in the KREEP geochemical reservoir (Barnes et al., 2016; McCubbin et al., 2015); however, these samples have experienced a range of secondary processes, including impact processes and secondary metasomatic events that could have overprinted their primordial Cl isotopic signatures (Elardo et al., 2012; Neal and Taylor, 1991; Shearer et al., 2015; Warren, 1988; Warren, 1993). In the present study, we determine the Cl-isotopic composition of the most pristine magnesian-suite sample, troctolite 76535, to place constraints on the Cl-isotopic composition of KREEP.

Magnesian suite troctolite 76535 was collected as a rake sample at station 6 during the Apollo 17 mission and was determined to have a confidence class of 9, indicating it is pristine with minimal evidence of post-crystallization impact processing (Warren, 1993). However, 76535 does exhibit evidence of post-cumulate metasomatism and/or metamorphism as it slowly cooled in the lunar crust (Elardo et al., 2012; McCallum and Schwartz, 2001; Shearer et al., 2015). Barnes et al. (2016) reported a Cl-isotopic composition of 31.6 ± 1.3‰ in apatite within the intercumulus regions of 76535. In addition to intercumulus apatite in 76535, apatite is present within a rare

holocrystalline olivine-hosted melt inclusion (Elardo et al., 2012; Dymek et al., 1975). Apatites within olivine-hosted melt inclusions in plutonic rocks from Mars have been shown to preserve the Cl-isotopic composition of their parental magmas even after the Cl-isotopic compositions of intercumulus apatite has been overprinted by metasomatism (Shearer et al., 2018). Therefore, we aim to determine the Cl-isotopic composition of both intercumulus apatite and apatite within an olivine-hosted melt inclusion in 76535 to constrain the Cl-isotopic composition of the 76535 magma and hence, the KREEP geochemical reservoir on the Moon.

Methods

Apollo thin section 76535,56 was chosen for this study because it was shown previously to have both intercumulus apatite and apatite within an olivine-hosted melt inclusion (e.g., Dymek et al., 1975; Elardo et al., 2012; McCallum and Schwartz, 2001). Given our access to sample maps, back-scattered electron images, and electron microprobe data on this sample from our previous work (e.g., Elardo et al., 2012; McCubbin et al., 2011), we did not seek to duplicate prior efforts. Consequently, we focused our analytical efforts on attaining new Cl-isotopic data for this sample. Melt inclusions within 76535 are rare, and to date we know of only a single olivine-hosted melt inclusion in our examination of two thin sections of 76535 (splits ,56 and ,159).

Nanoscale secondary ion mass spectrometry (NanoSIMS)

Apollo thin section 76535,56 was analyzed by nanoscale secondary ion mass spectrometry (NanoSIMS) in May of 2019. Both intercumulus apatite and apatite in the melt inclusion were analyzed. The Cl abundances of the target apatites were accurately determined by electron probe microanalysis prior to NanoSIMS (e.g., Elardo et al., 2012; McCubbin et al., 2011), therefore we did not determine Cl abundances of the apatites by NanoSIMS. The sample and reference materials were coated with ~8 nm of carbon to aid charge compensation during analysis.

The Cameca NanoSIMS 50L at NASA's Johnson Space Center (JSC) was used to measure the Cl-isotopic composition of apatite in 76535. We use delta notation to report our Cl isotope data where $\delta^{37}Cl = (({}^{37}Cl/{}^{35}Cl_{sample}/{}^{37}Cl/{}^{35}Cl_{standard}) - 1) \times 1000$ and SMOC = standard mean ocean chloride value (Kaufmann et al., 1984). A primary Cs^+ ion beam of ~5 pA current was used. The NanoSIMS 50L ion probe was operated in multi-collection mode and the negative secondary ions of ^{13}C, $^{16}O^1H$, ^{18}O, ^{30}Si, ^{35}Cl, and ^{37}Cl were collected simultaneously in electron multipliers. The mass spectrometer was tuned to a mass resolving power of ~9000 (Cameca definition), which allowed isobaric interferences between $^{16}O^1H$ and ^{17}O to be resolved.

The incident ion beam of ~500pA was rastered over ~400 μm^2 areas during ~10 minutes of pre-sputtering to clean the sample surface. The raster size was reduced to ~100 μm^2 area during analysis. Isotope images were collected at 256×256 pixels with a dwell time of ~200 seconds per image plane. Between 20 and 40 image planes were collected depending on the heterogeneity of each location as determined during pre-sputtering and initial tuning using real time isotope imaging. Cracks were easily identified based on correlated highs of C, OH, and Cl ions in real time isotope imaging.

Two well-characterized terrestrial apatites, Durango apatite from Mexico and apatite from Crystal Lode Pegmatite Mine in Colorado, U.S.A (fully described in McCubbin et al., 2012; McCubbin et al., 2010) were used in this work. The known Cl-isotopic values for Durango and Colorado apatites are 0.3 ‰ and 0.5 ‰, respectively (Zachary Sharp, Pers. Comm). Instrument mass fractionation of $^{37}Cl/^{35}Cl$ ratio was between 1 and 5 ‰ during the analytical session as determined on repeat measurements of Colorado apatite. When treated as an unknown, Durango apatite returned $\delta^{37}Cl$ compositions within 1 ‰ of its known value.

Image processing was performed using software designed by S. Messenger at JSC. This software allowed regions of interest to be selected within each compiled image and the isotopic composition to be determined using the above IMF values.

Results

We attained Cl-isotopic data on both intercumulus apatite and apatite within a single holocrystalline olivine-hosted melt inclusion in sample 76535,56. Backscattered electron (BSE) images of the apatites analyzed in this study, along with labels for NanoSIMS analysis spots, are provided in Figure 1. Previously published electron microprobe data on the intercumulus apatite and the apatite within an olivine-hosted melt inclusion indicate that the Cl abundances of apatite from the melt-inclusion apatite range from 1.26 to 1.29 wt.% Cl (Elardo et al., 2012), whereas the intercumulus apatite within 76535,56 ranges from 1.14 to 1.78 wt.% Cl (Elardo et al., 2012; McCubbin et al., 2011; Table S1). The electron microprobe data indicate the remainder of the volatile site in these apatites is occupied by fluorine (Elardo et al., 2012; McCubbin et al., 2011; Table S1), which is consistent with reported H_2O abundances in apatite from 76535 that are typically below 44 ppm H_2O (Barnes et al., 2014). A compilation of F-Cl-OH apatite compositions from intercumulus regions and an olivine-hosted melt inclusion in sample 76535,56 are shown in Figure 2. The Cl-isotopic compositions of the intercumulus apatite has an average value of 30.3 ± 1.1 ‰ (2σ), and the apatite within the olivine-hosted melt inclusion has an average Cl-isotopic composition of 28.3 ± 0.9 ‰ (2σ) (Table 1).

Discussion

The apatites within 76535,56 exhibit a limited range in their F-Cl-OH compositions, with most of the variation occurring along the F-Cl join (Figure 2). The F/Cl ratio of the apatite within the holocrystalline olivine-hosted melt inclusion overlaps with the highest F/Cl ratio of apatite

within the intercumulus region, although the intercumulus apatites exhibit a broader range of F/Cl ratios (Figure 2). The range in apatite compositions and extension to lower F/Cl ratio among the intercumulus apatite population is consistent with fractional crystallization of the intercumulus melt in an OH-poor system (Boyce et al., 2014; McCubbin and Ustunisik, 2018). The presence of more F-rich apatite within the melt inclusion could indicate that the melt inclusion underwent closer to equilibrium crystallization conditions where the apatites would have a limited compositional range with more fluorine-rich compositions compared to apatite that formed as a result of fractional crystallization (Piccoli and Candela, 2002; Boyce et al., 2014; McCubbin et al., 2016; Meurer and Boudreau, 1996). Overall, the apatites within 76535 do not exhibit any obvious evidence of degassing or assimilation of crustal fluids on the basis of their ranges in F-Cl-OH composition.

The Cl-isotopic compositions of apatite within the intercumulus regions of 76535 overlaps with the Cl-isotopic composition of apatite within the olivine-hosted melt inclusion in 76535 (Table 1). This observation indicates that the Cl-isotopic composition of the intercumulus apatite was not altered during the secondary metasomatic processes that produced the symplectite features in the intercumulus portions of 76535 (Ealrdo et al., 2012; McCallum and Schwartz, 2001). Furthermore, late-stage degassing of the troctolitic magma that formed 76535 is unlikely to have affected the Cl-isotopic composition of apatites within 76535 because it is a plutonic rock that formed within the lunar crust, and any degassing would have occurred at 200–250 MPa (McCallum and Schwartz, 2001). These crustal pressures are far from the conditions thought to facilitate Cl-isotopic fractionation by degassing (Sharp et al., 2010; Ustunisik et al., 2015). Furthermore, the concordance between the Cl isotopic composition of the intercumulus apatite and apatite in the olivine-hosted melt inclusion argues further against Cl-isotopic modification by late-

193 stage degassing given that the former crystallized in an open system and the latter crystallized in
194 a closed system.
195
196 **Cl-isotopic composition of KREEP**
197 Apatite in the olivine-hosted melt inclusion crystallized from melt that was trapped by a
198 growing cumulus olivine grain, hence the Cl-isotopic composition of that apatite may represent an
199 intrinsic feature of the KREEP-rich liquids that formed troctolite 76535. Of the three components
200 that are thought to have contributed to the parental liquids of troctolite 76535 (i.e., early Mg-rich
201 LMO cumulates, ferroan anorthosites, and KREEP), KREEP is the most Cl-rich as it represents
202 the primary Cl reservoir on the Moon (McCubbin et al., 2015; Boyce et al., 2018). Therefore, we
203 infer that the Cl isotopic composition of the apatite within the olivine-hosted melt inclusion
204 represents the Cl-isotopic composition of the KREEP reservoir. Moreover, we conclude that the
205 isotopic composition of KREEP was already fractionated to values between 28 ‰ and 30 ‰ by
206 4.31 Ga (Borg et al., 2015), consistent with hypotheses for the origin of ^{37}Cl-enrichment of
207 KREEP-rich lunar samples that call upon either degassing of chlorides from the LMO (Boyce et
208 al., 2015) or degassing of melt exposed to the lunar surface during an early crust-breaching impact
209 within the Procellerum KREEP Terrane (Barnes et al., 2016).
210 One caveat to this interpretation is that we only know of a single apatite-bearing olivine-
211 hosted melt inclusion in 76535. Although olivine is one of the best hosts for preserving melt
212 inclusions (Roedder, 1979; Shearer et al., 2018; Veksler, 2006), and the apatite-bearing melt
213 inclusion does not appear to have been obviously breached, we cannot rule out that possibility
214 entirely and efforts to find additional melt inclusions in 76535 would aid in constraining the
215 geochemistry of KREEP.

Origin of Cl-isotopic variation in lunar samples

The Cl-isotopic value for KREEP reported in this study falls within the broad range of values that have been reported for lunar samples, which range from -4‰ to +81‰ (Barnes et al., 2019; Barnes et al., 2016; Boyce et al., 2015; Potts et al., 2018; Sharp et al., 2010; Shearer et al., 2014; Stephant et al., 2019; Tartèse et al., 2014a; Treiman et al., 2014; Wang et al., 2019). The lower values of this range are associated with the most KREEP-poor lunar samples (Barnes et al., 2019; Barnes et al., 2016; Boyce et al., 2018; Boyce et al., 2015; Sharp et al., 2010; Wang et al., 2019), hence the low values may represent the Cl-isotopic composition of the primordial lunar mantle (Barnes et al., 2019; Barnes et al., 2016; Boyce et al., 2018; Sharp et al., 2010). The lunar mantle values overlap with the Cl-isotopic compositions of Earth, Mars, 4 Vesta, and chondrites (Barrett et al., 2019; Sarafian et al., 2017; Sharp et al., 2007; Sharp and Draper, 2013; Williams et al., 2016). For lunar samples with Cl-isotopic compositions exceeding the value for KREEP, secondary impact processes have affected many of them (e.g., Barnes et al., 2019; Treiman et al., 2014; Wang et al., 2019). Degassing of metal chlorides in a vacuum may promote the preferential loss of ^{35}Cl to the vapor phase, which would leave the residual impact melt with high $\delta^{37}Cl$ values (Sharp et al., 2010; Ustunisik et al., 2015); however, the efficacy of this mechanism has yet to be evaluated in detail through experiments. Magmatic degassing has also been proposed as a possible explanation of Cl-isotopic variation in lunar basalts (Sharp et al., 2010). This process cannot be ruled out and may complicate interpretations of Cl isotopes for lunar samples that have Cl-isotopic compositions that are intermediate between the lunar mantle and KREEP. For these samples, a coordinated approach combining textural context and chemical analyses will be required, akin to efforts that aimed to understand complex H-isotopic systematics in lunar samples (e.g., Tartèse et al., 2014b).

Implications

The presence of olivine-hosted melt inclusions within one of the most pristine KREEP-rich rocks from the highlands magnesian suite provides a new opportunity to characterize the geochemistry of KREEP, the most enigmatic geochemical reservoir on the Moon. In particular, a broader analysis of stable isotopic compositions of highly and moderately volatile elements could provide an unprecedented advancement in our characterization of the KREEP reservoir and of volatile depletion processes during planetary formation, more broadly. These studies should focus on systems that can be reasonably preserved within olivine-hosted melt inclusions. For example, it would be inadvisable to evaluate the H-isotopic composition of KREEP from olivine-hosted melt inclusions in 76535 given its protracted cooling history, and the infidelity of melt inclusions when it comes to preservation of H_2O and H in slowly cooled samples (e.g., Bucholz et al., 2013; Gaetani et al., 2012; Ni et al., 2019; Ni et al., 2017). However, Zn, K, Rb, and S isotopic data may be preserved within the inclusions and could provide valuable insights into the geochemistry of the KREEP reservoir and volatile-depletion processes during magma ocean crystallization.

Acknowledgements

We are grateful to the curatorial staff at NASA Johnson Space Center for allocation of sample 76535,56. Apollo sample curation is funded by NASA and curated by the Astromaterials Acquisition and Curation Office at NASA Johnson Space Center. We are grateful to Bruce Watson for the editorial handling of this manuscript and to Nicholas Tailby and an anonymous reviewer for comments that improved the quality of this work. FMM was supported by NASA's Planetary Science Research Program during this work. JJB was supported by the NASA Postdoctoral Program during this work.

References

Barnes, J.J., Tartese, R., Anand, M., McCubbin, F.M., Franchi, I.A., Starkey, N.A., and Russell, S.S. (2014) The origin of water in the primitive Moon as revealed by the lunar highlands samples. Earth and Planetary Science Letters, 390, 244-252.

Barnes, J.J., Tartèse, R., Anand, M., McCubbin, F.M., Neal, C.R., and Franchi, I.A. (2016) Early degassing of lunar urKREEP by crust-breaching impact(s). Earth and Planetary Science Letters, 447, 84-94.

Barnes, J.J., Franchi, I.A., McCubbin, F.M., and Anand, M. (2019) Multiple volatile reservoirs on the Moon revealed by the isotopic composition of chlorine in lunar basalts. Geochimica et Cosmochimica Acta, 266, 144-162.

Barrett, T.J., Barnes, J.J., Anand, M., Franchi, I.A., Greenwood, R.C., Charlier, B.L.A., Zhao, X., Moynier, F., and Grady, M.M. (2019) Investigating magmatic processes in the early Solar System using the Cl isotopic systematics of eucrites. Geochimica et Cosmochimica Acta, 266, 582-597.

Borg, L.E., Gaffney, A.M., and Shearer, C.K. (2015) A review of lunar chronology revealing a preponderance of 4.34-4.37 Ga ages. Meteoritics & Planetary Science, 50, 715-732.

Boyce, J.W., Tomlinson, S.M., McCubbin, F.M., Greenwood, J.P., and Treiman, A.H. (2014) The lunar apatite paradox. Science, 344, 400-402.

Boyce, J.W., Treiman, A.H., Guan, Y., Ma, C., Eiler, J.M., Gross, J., Greenwood, J.P., and Stolper, E.M. (2015) The chlorine isotope fingerprint of the lunar magma ocean. Science Advances, 1, DOI: 10.1126/sciadv.1500380.

Boyce, J.W., Kanee, S.A., McCubbin, F.M., Barnes, J.J., Bricker, H., and Treiman, A.H. (2018) Chlorine isotopes in the low-Ti Basalts, and the early loss of volatiles from the Earth-Moon system. Earth and Planetary Science Letters, 500, 205-214.

Bucholz, C.E., Gaetani, G.A., Behn, M.D., and Shimizu, N. (2013) Post-entrapment modification of volatiles and oxygen fugacity in olivine-hosted melt inclusions. Earth and Planetary Science Letters, 374, 145-155.

Canup, R.M., and Asphaug, E. (2001) Origin of the Moon in a giant impact near the end of the Earth's formation. Nature, 412, 708-712.

Charlier, B., Grove, T.L., Namur, O., and Holtz, F. (2018) Crystallization of the lunar magma ocean and the primordial mantle-crust differentiation of the Moon. Geochimica et Cosmochimica Acta, 234, 50-69.

Connelly, J.N., Bizzarro, M., Krot, A.N., Nordlund, A., Wielandt, D., and Ivanova, M.A. (2012) The absolute chronology and thermal processing of solids in the solar protoplanetary disk. Science, 338, 651-655.

Day, J.M.D. and Moynier, F. (2014) Evaporative fractionation of volatile stable isotopes and their bearing on the origin of the Moon. Philosophical Transactions of the Royal Society a-Mathematical Physical and Engineering Sciences, 372, doi.org/10.1098/rsta.2013.0259.

Day, J.M.D., van Kooten, E.M.M.E., Hofmann, B.A., and Moynier, F. (2020) Mare basalt meteorites, magnesian-suite rocks and KREEP reveal loss of zinc during and after lunar formation. Earth and Planetary Science Letters, 531, 115998.

Dhaliwal, J.K., Day, J.M.D., and Moynier, F. (2018) Volatile element loss during planetary magma ocean phases. Icarus, 300, 249-260.

Dymek R. F., Albee A. L. and Chodos A. A. (1975) Comparative petrology of lunar cumulate rocks of possible primary origin: dunite 72415, troctolite 76535, norite 78235, and anorthosite 62237. 6th Lunar Sci. Conf. 301–341.

Elardo, S.M., Draper, D.S., and Shearer, C.K. (2011) Lunar magma ocean crystallization revisited: Bulk composition, early cumulate mineralogy, and the source regions of the highlands Mg-suite. Geochimica et Cosmochimica Acta, 75, 3024-3045.

Elardo, S.M., McCubbin, F.M., and Shearer, C.K. (2012) Chromite symplectites in Mg-suite troctolite 76535 as evidence for infiltration metasomatism of a lunar layered intrusion. Geochimica et Cosmochimica Acta, 87, 154-177.

Elkins-Tanton, L.T. and Grove, T.L. (2011) Water (hydrogen) in the lunar mantle: Results from petrology and magma ocean modeling. Earth and Planetary Science Letters, 307, 173-179.

Gaetani, G.A., O'Leary, J.A., Shimizu, N., Bucholz, C.E., and Newville, M. (2012) Rapid reequilibration of H_2O and oxygen fugacity in olivine-hosted melt inclusions. Geology, 40, 915-918.

Hartmann, W.K. and Davis, D.R. (1975) Satellite-sized planetesimals and lunar origin. Icarus, 24, 504-515.

Hauri, E.H., Saal, A.E., Rutherford, M.J., and Van Orman, J.A. (2015) Water in the Moon's interior: Truth and consequences. Earth and Planetary Science Letters, 409, 252-264.

Hess, P.C. (1994) Petrogenesis of lunar troctolites. Journal of Geophysical Research-Planets, 99, 19083-19093.

Hess, P.C., and Parmentier, E.M. (1995) A model for the thermal and chemical evolution of the Moon's interior: Implications for the onset of mare volcanism. Earth and Planetary Science Letters, 134, 501-514.

Kato, C., Moynier, F., Valdes, M.C., Dhaliwal, J.K., and Day, J.M.D. (2015) Extensive volatile loss during formation and differentiation of the Moon. Nature Communications, 6, doi.org/10.1038/ncomms8617.

Kaufmann, R., Long, A., Bentley, H., and Davis, S. (1984) Natural chlorine isotope variations. Nature, 309, 338-340.
Lin, Y., Tronche, E.J., Steenstra, E.S., and van Westrenen, W. (2017) Experimental constraints on the solidification of a nominally dry lunar magma ocean. Earth and Planetary Science Letters, 471, 104-116.
Lock, S.J., Stewart, S.T., Petaev, M.I., Leinhardt, Z., Mace, M.T., Jacobsen, S.B., and Cuk, M. (2018) The origin of the Moon within a terrestrial synestia. Journal of Geophysical Research-Planets, 123, 910-951.
McCallum, I.S. and Schwartz, J.M. (2001) Lunar Mg suite: Thermobarometry and petrogenesis of parental magmas. Journal of Geophysical Research-Planets, 106, 27969-27983.
McCubbin, F.M. and Ustunisik, G. (2018) Experimental investigation of F and Cl partitioning between apatite and Fe-rich basaltic melt at 0 GPa and 950-1050 ^{o}C: Evidence for steric controls on apatite-melt exchange equilibria in OH-poor apatite. American Mineralogist, 103, 1455-1467.
McCubbin, F.M., Steele, A., Hauri, E.H., Nekvasil, H., Yamashita, S., and Hemley, R.J. (2010) Nominally hydrous magmatism on the Moon. Proceedings of the National Academy of Sciences of the United States of America, 27, 11223-11228.
McCubbin, F.M., Jolliff, B.L., Nekvasil, H., Carpenter, P.K., Zeigler, R.A., Steele, A., Elardo, S.M., and Lindsley, D.H. (2011) Fluorine and chlorine abundances in lunar apatite: Implications for heterogeneous distributions of magmatic volatiles in the lunar interior. Geochimica et Cosmochimica Acta, 75, 5073-5093.
McCubbin, F.M., Hauri, E.H., Elardo, S.M., Vander Kaaden, K.E., Wang, J., and Shearer, C.K. (2012) Hydrous melting of the martian mantle produced both depleted and enriched shergottites. Geology, 40, 683-686.
McCubbin, F.M., Kaaden, K.E.V., Tartèse, R., Klima, R.L., Liu, Y., Mortimer, J., Barnes, J.J., Shearer, C.K., Treiman, A.H., Lawrence, D.J., Elardo, S.M., Hurley, D.M., Boyce, J.W., and Anand, M. (2015) Magmatic volatiles (H, C, N, F, S, Cl) in the lunar mantle, crust, and regolith: Abundances, distributions, processes, and reservoirs. American Mineralogist, 100, 1668-1707.
McCubbin, F.M., Boyce, J.W., Srinivasan, P., Santos, A.R., Elardo, S.M., Filiberto, J., Steele, A., and Shearer, C.K. (2016) Heterogeneous distribution of H_2O in the martian interior: Implications for the abundance of H_2O in depleted and enriched mantle sources. Meteoritics & Planetary Science, 51, 2036-2060.
Meurer, W.P. and Boudreau, A.E. (1996) An evaluation of models of apatite compositional variability using apatite from the middle banded series of the Stillwater Complex, Montana. Contributions to Mineralogy and Petrology, 125, 225–236.
Neal, C.R. and Taylor, L.A. (1991) Evidence for metasomatism of the lunar highlands and the origin of whitlockite. Geochimica et Cosmochimica Acta, 55, 2965-2980.
Ni, P., Zhang, Y., and Guan, Y. (2017) Volatile loss during homogenization of lunar melt inclusions. Earth and Planetary Science Letters, 478, 214-224.
Ni, P., Zhang, Y., Chen, S., and Gagnon, J. (2019) A melt inclusion study on volatile abundances in the lunar mantle. Geochimica et Cosmochimica Acta, 249, 17-41.
Piccoli, P.M., and Candela, P.A. (2002) Apatite in igneous systems. In M.J. Kohn, J. Rakovan, and J.M. Hughes, Eds., Phosphates: Geochemical, Geobiological, and Materials Importance, 48, p. 255-292. Reviews in Mineralogy and Geochemistry, Mineralogical Society of America, Washington, DC.
Potts, N.J., Barnes, J.J., Tartese, R., Franchi, I.A., and Anand, M. (2018) Chlorine isotopic compositions of apatite in Apollo 14 rocks: Evidence for widespread vapor-phase metasomatism on the lunar nearside similar to 4 billion years ago. Geochimica et Cosmochimica Acta, 230, 46-59.
Rapp, J.F. and Draper, D.S. (2018) Fractional crystallization of the lunar magma ocean: Updating the dominant paradigm. Meteoritics & Planetary Science, 53, 1432-1455.
Ringwood, A.E. and Kesson, S.E. (1976) A dynamic model for mare basalt petrogenesis. Proceedings of the 7th Lunar and Planetary Science Conference, 7, 1697-1722.
Roedder, E. (1979) Origin and significance of magmatic inclusions. Bulletin de Mineralogie, 102, 487-510.
Sarafian, A.R., John, T., Roszjar, J., and Whitehouse, M.J. (2017) Chlorine and hydrogen degassing in Vesta's magma ocean. Earth and Planetary Science Letters, 459, 311-319.
Sharp, Z.D. and Draper, D.S. (2013) The chlorine abundance of Earth: Implications for a habitable planet. Earth and Planetary Science Letters, 369-370, 71-77.
Sharp, Z.D., Barnes, J.D., Brearley, A.J., Chaussidon, M., Fischer, T.P., and Kamenetsky, V.S. (2007) Chlorine isotope homogeneity of the mantle, crust and carbonaceous chondrites. Nature, 446, 1062-1065.
Sharp, Z.D., Shearer, C.K., McKeegan, K.D., Barnes, J.D., and Wang, Y.Q. (2010) The chlorine isotope composition of the Moon and implications for an anhydrous mantle. Science, 329, 1050-1053.
Shearer, C.K., and Papike, J. (2005) Early crustal building processes on the moon: Models for the petrogenesis of the magnesian suite. Geochimica et Cosmochimica Acta, 69, 3445-3461.

Shearer, C.K., Hess, P.C., Wieczorek, M.A., Pritchard, M.E., Parmentier, E.M., Borg, L.E., Longhi, J., Elkins-Tanton, L.T., Neal, C.R., Antonenko, I., Canup, R.M., Halliday, A.N., Grove, T.L., Hager, B.H., Lee, D.C., and Wiechert, U. (2006) Thermal and magmatic evolution of the moon. In B.L. Jolliff, M.A. Wieczorek, C.K. Shearer and C.R. Neal, Eds., New Views of the Moon, 60, p. 365-518. Reviews in Mineralogy and Geochemistry, Mineralogical Society of America, Chantilly, VA.

Shearer, C.K., Sharp, Z.D., Burger, P.V., McCubbin, F.M., Provencio, P.P., Brearley, A.J., and Steele, A. (2014) Chlorine distribution and its isotopic composition in "rusty rock" 66095. Implications for volatile element enrichments of "rusty rock" and lunar soils, origin of "rusty" alteration, and volatile element behavior on the Moon. Geochimica et Cosmochimica Acta, 139, 411-433.

Shearer, C.K., Elardo, S.M., Petro, N.E., Borg, L.E., and McCubbin, F.M. (2015) Origin of the lunar highlands Mg-suite: An integrated petrology, geochemistry, chronology, and remote sensing perspective. American Mineralogist, 100, 294-325.

Shearer, C.K., Messenger, S., Sharp, Z.D., Burger, P.V., Nguyen, A.N., and McCubbin, F.M. (2018) Distinct Chlorine Isotopic Reservoirs on Mars. Implications for character, extent and relative timing of crustal interaction with mantle-derived magmas, evolution of the martian atmosphere, and the building blocks of an early Mars. Geochimica et Cosmochimica Acta, 234, 24-36.

Snyder, G.A., Taylor, L.A., and Neal, C.R. (1992) A chemical-model for generating the sources of mare basalts: Combined equilibrium and fractional crystallization of the lunar magmasphere. Geochimica et Cosmochimica Acta, 56, 3809-3823.

Stephant, A., Anand, M., Zhao, X., Chan, Q.H.S., Bonifacie, M., and Franchi, I.A. (2019) The chlorine isotopic composition of the Moon: Insights from melt inclusions. Earth and Planetary Science Letters, 523, 115715.

Tartèse, R., Anand, M., Joy, K.H., and Franchi, I.A. (2014a) H and Cl isotope systematics of apatite in brecciated lunar meteorites Northwest Africa 4472, Northwest Africa 773, Sayh al Uhaymir 169, and Kalahari 009. Meteoritics & Planetary Science, 49, 2266-2289.

Tartèse, R., Anand, M., McCubbin, F.M., Elardo, S.M., Shearer, C.K., and Franchi, I.A. (2014b) Apatites in lunar KREEP basalts: The missing link to understanding the H isotope systematics of the Moon. Geology, 42, 363-366.

Taylor, S.R., Taylor, G.J., and Taylor, L.A. (2006) The Moon: A Taylor perspective. Geochimica et Cosmochimica Acta, 70, 5904-5918.

Touboul, M., Kleine, T., Bourdon, B., Palme, H., and Wieler, R. (2007) Late formation and prolonged differentiation of the Moon inferred from W isotopes in lunar metals. Nature, 450, 1206-1209.

Treiman, A.H., Boyce, J.W., Gross, J., Guan, Y.B., Eiler, J.M., and Stolper, E.M. (2014) Phosphate-halogen metasomatism of lunar granulite 79215: Impact-induced fractionation of volatiles and incompatible elements. American Mineralogist, 99, 1860-1870.

Ustunisik, G., Nekvasil, H., Lindsley, D.H., and McCubbin, F.M. (2015) Degassing pathways of Cl-, F-, H-, and S-bearing magmas near the lunar surface: Implications for the composition and Cl isotopic values of lunar apatite. American Mineralogist, 100, 1717-1727.

Veksler, I.V. (2006) Crystallized melt inclusions in gabbroic rocks. In J.D. Webster, Eds., Melt Inclusions in Plutonic Rocks, 36, p. 99-122. Mineralogical Association of Canada, Montreal.

Wang, K. and Jacobsen, S.B. (2016) Potassium isotopic evidence for a high-energy giant impact origin of the Moon. Nature, 538, 487-490.

Wang, Y., Hsu, W., and Guan, Y. (2019) An extremely heavy chlorine reservoir in the Moon: Insights from the apatite in lunar meteorites. Scientific Reports, 9, 5727.

Warren, P.H. (1988) The origin of pristine KREEP: Effects of mixing between urKREEP and the magmas parental to the Mg-rich cumulates. Proceedings of Lunar and Planetary Science Conference, 18, 233-241.

-. (1993) A concise compilation of petrologic information on possibly pristine nonmare Moon rocks. American Mineralogist, 78, 360-376.

Warren, P.H. and Wasson, J.T. (1979) Origin of KREEP. Reviews of Geophysics, 17, 73-88.

Wieczorek, M.A., Jolliff, B.L., Khan, A., Pritchard, M.E., Weiss, B.P., Williams, J.G., Hood, L.L., Righter, K., Neal, C.R., Shearer, C.K., McCallum, I.S., Tompkins, S., Hawke, B.R., Peterson, C., Gillis, J.J., and Bussey, B. (2006) The constitution and structure of the lunar interior. In B.L. Jolliff, M.A. Wieczorek, C.K. Shearer and C.R. Neal, Eds., New Views of the Moon, 60, p. 221-364. Reviews in Mineralogy and Geochemistry, Mineralogical Society of America, Chantilly, VA.

Williams, J.T., Shearer, C.K., Sharp, Z.D., Burger, P.V., McCubbin, F.M., Santos, A.R., Agee, C.B., and McKeegan, K.D. (2016) The chlorine isotopic composition of martian meteorites Part 1: Chlorine isotope composition

of martian mantle and crustal reservoirs and their interactions. Meteoritics & Planetary Science, 51, 2092-2110.

Table 1. Cl-isotopic data for apatites within 76535,56

Apatite ID	ROI#	δ^{37}Cl (‰)	2s (‰)	Comment
1a	1	30.2	1.4	Cl-rich area
1a	2	30.9	1.1	Entire apatite grain for comparison to ROI 1
1b	1	29.6	1.1	Cl even across area imaged
MIAp1	1	28.4	0.8	Most even area within this ROI and furthest from cracks and edges
MIAp2	1	28.2	0.9	3D ROI as image shifted during analysis

This is a preprint, the final version is subject to change, of the American Mineralogist (MSA)
Cite as Authors (Year) Title. American Mineralogist, in press.
DOI: https://doi.org/10.2138/am-2020-7467

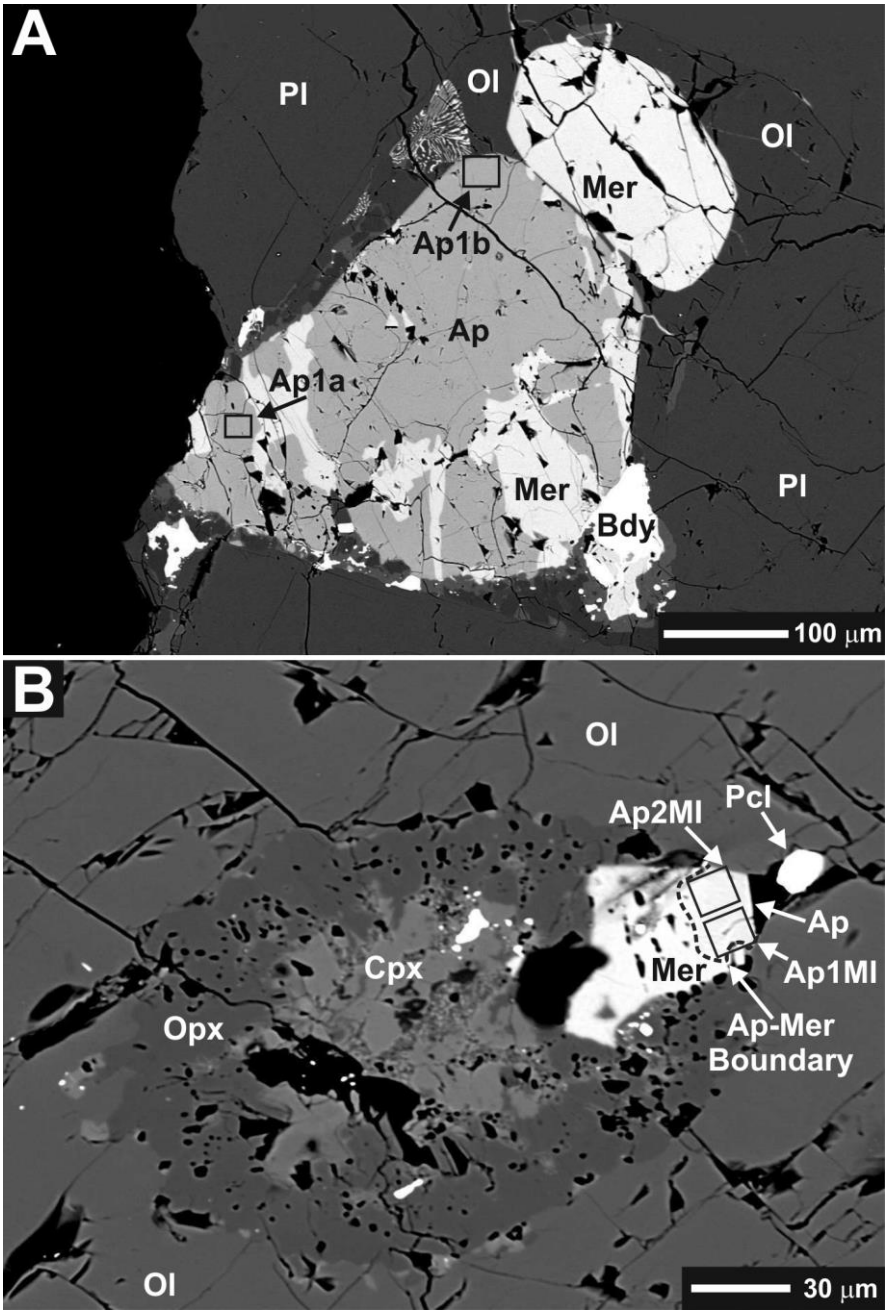

Figure 1. Back-scattered electron images of A) Intercumulus apatite and B) apatite within holocrystalline olivine-hosted melt inclusion from Apollo sample 76535,56. Black-bordered rectangles outline NanoSIMS analysis spots in both images, and a dotted line outlines the boundary between apatite and merrillite in Figure 1B. Phases present are identified, and the phase abbreviations are indicated as follows: Ap = apatite, Cpx = clinopyroxene, Mer = merrillite, Ol = olivine, Opx = orthopyroxene, Pcl = pyrochlore, Pl = plagioclase. BSE images adapted from Elardo et al. (2012).

This is a preprint, the final version is subject to change, of the American Mineralogist (MSA)
Cite as Authors (Year) Title. American Mineralogist, in press.
DOI: https://doi.org/10.2138/am-2020-7467

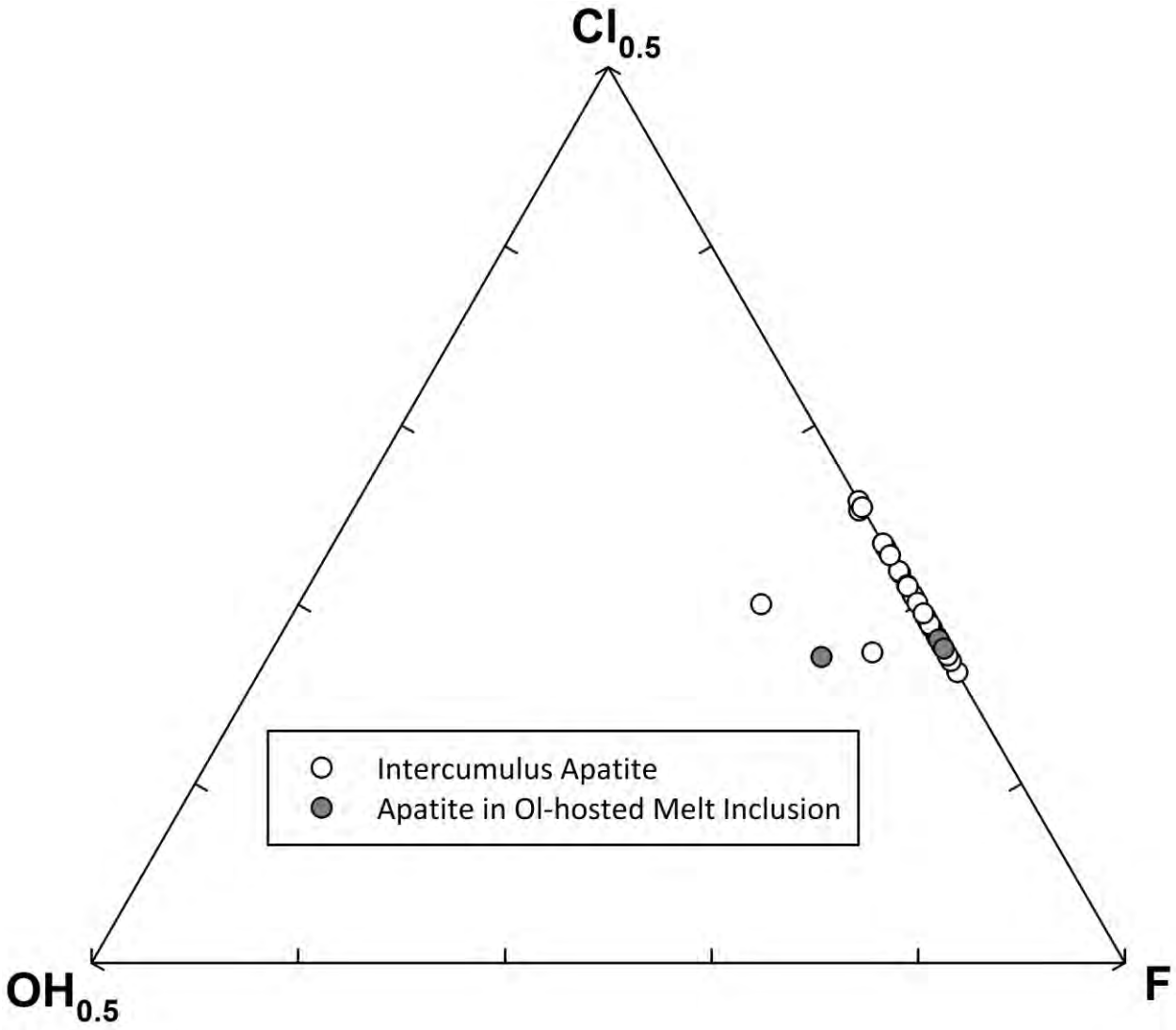

Figure 2. Truncated ternary plot of apatite X-site occupancy (mol%) from 76535, 56 from McCubbin et al., (2011) and Elardo et al. (2012). OH was not directly measured, so it was calculated assuming 1 – F – Cl = OH. EPMA data yielding (F + Cl) > 1 atom are plotted along the OH-free join assuming 1 – Cl = F.